JOURNAL OF MATERIALS SCIENCE 26 (1991) 3073–3080

Cellulosic solid films exhibiting cholesteric liquid crystalline order

Part I *Tensile creep in vacuo for ethyl cellulose and hydroxypropyl cellulose*

SHINICHI SUTO, TAKAO IWAYA, YUTAKA OHNO, MIKIO KARASAWA
Department of Polymer Chemistry, Faculty of Engineering, Yamagata University, Jonan 4-3-16, Yonezawa, Yamagata, 992, Japan

Ethyl cellulose (EC) and hydroxypropyl cellulose (HPC) films were cast under different conditions and were observed optically. The creep behaviour of those films was determined *in vacuo* as a function of applied stress or temperature and was analysed on the basis of the Eyring thermally activated process.

EC and HPC films cast from liquid crystal-forming systems remained cholesteric liquid crystalline order (the cholesteric sense was different in each case), whereas EC film cast from non-liquid crystal system (benzene) had no liquid crystalline order and was amorphous.

The Eyring activated process could be applied to the creep behaviour of our films and activated parameters could be evaluated. The activated volume V was of the order of 1 nm^3 and greatly depended on the casting conditions and testing temperature. The value of V tended to decrease as the liquid crystalline order increased. The value of V was smaller than the size of liquid crystalline domain.

1. Introduction

Many cellulose derivatives form both lyotropic and thermotropic liquid crystals. The solid cellulosic films prepared at suitable conditions remain of liquid crystalline order [1–3]. We have noted that the cellulosic solid films exhibiting the cholesteric liquid crystalline order have potential uses as gas- or liquid-separation filters [4, 5]. When we discuss the applicability of those cellulosic films to the separation filters, we need fundamental data on both the gas- or liquid-permeability and morphology of the films prepared. Takahashi *et al.* [6], Shimamura [7], Horio *et al.* [8], and Nishio *et al.* [9–11] have investigated the morphology of the cellulosic lyotropic and thermotropic liquid crystals and have reported that the morphology of the films was affected by the conditions of preparation such as shear rate.

In this study, we focus on the creep behaviour of ethyl cellulose (EC) and hydroxypropyl cellulose (HPC) films which exhibit liquid crystalline order. The study of the creep behaviour is of interest from two points of view. First, creep behaviour itself should be one of the important characteristics examined, when we discuss the applicability of the films to the filters. Secondly, on the basis of the Eyring activated process [12], some activated parameters can be evaluated experimentally using the creep data [13, 14]. Therefore, if the Eyring activated process can be applied to the creep behaviour of the solid films which exhibit the liquid crystalline order, we can evaluate the activated parameters of liquid crystals. The evaluation of the parameters may provide valuable information on the liquid crystalline domain behaviour during deformation.

Recently, Ward *et al.* [15, 17] have investigated the creep behaviour of polyethylene on the basis of the Eyring thermally activated process and have reported the activated parameters. Some researchers [18, 19] have investigated the creep behaviour of the liquid crystalline fibre, Kevlar. We have also investigated the effect of casting conditions on the creep behaviour for EC films [20]. No one has, however, investigated the creep of liquid crystalline fibres and films on the basis of the Eyring process. Very recently, we have tried to apply the Eyring process to the creep behaviour of HPC films cast from liquid crystalline solutions and have successfully evaluated the activated parameters [21]. We need, however, to determine whether the Eyring process is valid for other liquid crystalline films or not.

In the present paper, we first prepared EC films and confirmed that the resultant films exhibit the cholesteric liquid crystalline order by polarized optical microscopy and circular dichroism. Secondly, we determined the creep behaviour of the EC films as a function of stress and temperature, applied the Eyring process to the behaviour, evaluated the activated parameters, and finally, discussed the dependence of those parameters on the casting conditions, comparing the data of HPC and EC films. Cellulosics are

0022–2461/91 $03.00 + .12

hygroscopic and hence the creep behaviour was determined *in vacuo* to eliminate the influence of moisture.

2. Analysis

The creep behaviour on the basis of the Eyring activated process [12] is mainly characterized by two parameters, namely, activated volume V and activated energy ΔU [13]. We need data regarding the dependence of the creep behaviour on both applied stress and temperature to evaluate those parameters. First, creep strain (ε) is plotted against time (t) at given stresses and temperatures. The strain rate ($\dot{\varepsilon}$) at given times is obtained by employing graphical differentiation method. The logarithm of the strain rate $\dot{\varepsilon}$ is plotted against strain ε – the so-called Sherby–Dorn plot [13]. With respect to the plot, the strain rate generally decreases with strain and ultimately attains a constant level (constant plateau strain rate $\dot{\varepsilon}_p$) at each applied stress and temperature.

Ward *et al.* [15] have proposed the following relation

$$\log \dot{\varepsilon}_p = \log(\dot{\varepsilon}_0/2) - \frac{\Delta U}{2.3kT} + \frac{\sigma V}{2.3kT} \quad (1)$$

where $\dot{\varepsilon}_0$ is constant, k the Boltzmann constant, T absolute temperature, and σ applied stress.

When the plot of $\log \dot{\varepsilon}_p$ against σ at given temperatures is a straight line of a slope of $(V/2)3kT$, the value of V can be evaluated.

Equation 1 can be rewritten as the following

$$\log \dot{\varepsilon}_p = \log(\dot{\varepsilon}_0/2) - \frac{(\Delta U - \sigma V)}{2.3kT} \quad (2)$$

When a plot of $\log \dot{\varepsilon}_p$ against $1/T$ at given stress is a straight line of slope $-(\Delta U - \sigma V)/2.3kT$, ΔU can be obtained because the values of V and σ are known. It is, however, noteworthy that the value of V is not constant over the range of temperature measured and the average value of V is used, consequently, the value of ΔU obtained is an average one.

3. Experimental procedure

3.1. Samples

Commercial reagent grade ethyl cellulose was used. Hydroxypropyl cellulose was also used for the comparison with data of EC. The characteristics of those cellulosics are shown in Table I. Molecular weights were determined in THF at 25 °C by means of GPC. Degrees of substitution of EC [22] and molar substitution of HPC [23] were determined by means of NMR.

TABLE I Molecular characteristics of cellulose derivatives used

Polymer code	$\bar{M}_w$	$\bar{M}_n$	DS	MS
EC-1	18.7×10^4	5.86×10^4	2.49	—
EC-2	13.5	4.31	2.48	—
EC-3	12.3	3.78	2.52	—
HPC	11.7	5.29	—	4.25

Commercial reagent grade m-cresol, benzene, and N,N-dimethylacetamide (DMA) were used.

3.2. Preparation of concentrated solutions

50 wt % solution of EC in m-cresol, 10 wt % solution of EC in benzene, and 20 wt % solution of HPC in DMA were prepared by storing in refrigerator (*ca.* 7 °C) for 3 to 4 months. EC/m-cresol [5] and HPC/DMA [24] systems form liquid crystals above 35 and 48 wt % at 25 °C, respectively; 50 wt % solution of EC in m-cresol is a single-phase liquid crystal and 20 wt % solution of HPC in DMA is isotropic. On the other hand, EC solution in benzene forms no liquid crystal.

3.3. Preparation of solid films

EC films and a HPC film were cast at room temperature (*ca.* 25 °C) and another HPC film was cast at − 18 °C *in vacuo*. The conditions and abbreviations of the resultant films are shown in Table II. In the case of casting at room temperature, each solution was spread on a glass plate over mercury. After about one week the resultant transparent film was peeled from the plate, dried *in vacuo* at 40 °C for about 24 h, and stored in a desiccator over silica gel at room temperature. In the case of casting at − 18 °C for HPC system, the solution (20 wt %) was spread on the glass plate. After about 4 days at room temperature, the surface of the solution changed from being transparent to being luminescent, then, the glass plate containing the solution was stored in a desiccator and the desiccator was transferred into the refrigerator (− 18 °C) and vacuumed. After about 3 weeks the luminescence of the surface disappeared. The transparent solid film was peeled, dried *in vacuo* at 40 °C, and stored in the desiccator at room temperature.

3.4. Polarized microscopical observation of cast films

An Olympus polarized microscope equipped camera was used to observe and to photograph the texture of the cast films. The magnification was 150 times.

TABLE II Cast conditions for EC and HPC films

Film code	Polymer code[a]	Initial concentration (wt %)	Solvent	Temperature (°C)
EC-A	EC-1	50	m-cresol	25
EC-B	EC-2	50	m-cresol	25
EC-C	EC-3	50	m-cresol	25
EC-D	EC-2	10	benzene	25
HPC-A	HPC	20	DMA[b]	25 → − 18 °C[c]
HPC-B	HPC	20	DMA	25

[a] See Table I.
[b] N,N-dimethylacetamide.
[c] *In vacuo*.

3.5. Circular dichroism (CD) of cast films

The selective reflectance of circularly polarized light was detected by circular dichroism with a Jasco J-40S automatic recording spectropolarimeter (Japan Spectroscopic Co. Ltd.) at room temperature in the wavelength range of 200 to 700 nm.

3.6. Small-angle light scattering (SALS) of cast films

Light scattering patterns were recorded using He–Ne gas laser (wavelength: 632.8 nm) as a polarized monochromatic light source.

3.7. Tensile creep

The specimen for creep test was cut along a line parallel to a longside of the cast film, which was similar to the spread direction of the concentrated solution. The size of the specimen was *ca.* 70 to 100 μm thick × 4 cm long × 0.15 cm wide. Polarized microscopical observation confirmed that the specimen had no macroscopic defects (air-void, crack, etc.).

The apparatus used is shown schematically in Fig. 1. The specimen was placed in a glass vessel and the vessel was evacuated at a given temperature for about 2 h; the distance between the fixed jaws was 2 cm and the reduced pressure was about 2.7 Pa. First, the load and lower fixed jaw were placed at the bottom of the vessel and the specimen was unloaded.

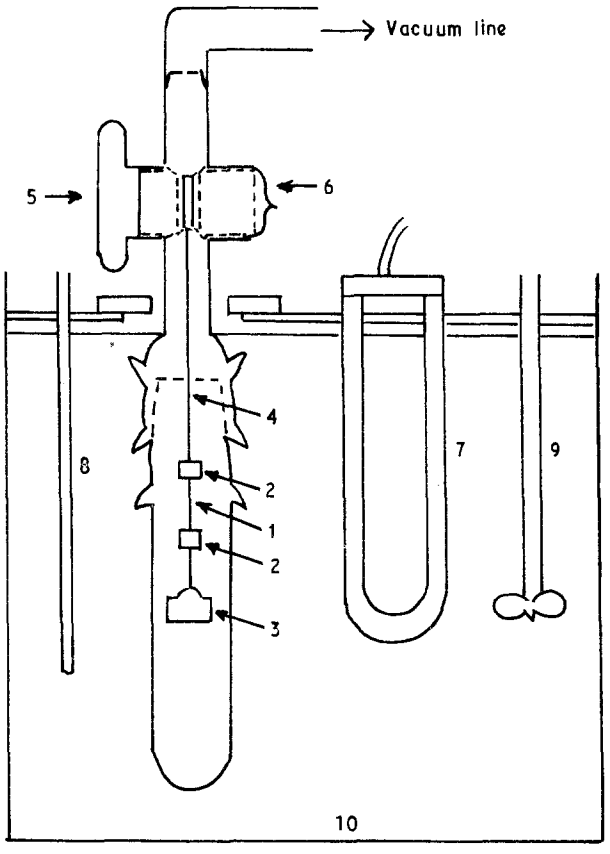

Figure 1 Schematic diagram of apparatus for measuring tensile creep under vacuum. (1 specimen, 2 fixed jaw, 3 load, 4 cotton yarn, 5 glass plug, 6 vacuum stopcock, 7 heater, 8 thermosensor, 9 stirrer, 10 oil or water bath)

After about 2 h, we turned a glass plug with a U-shaped groove as quickly and smoothly as possible; the cotton yarn which suspends the specimen and load was wounded up around the plug; and finally the specimen was subjected to a constant load. The amount of elongation was evaluated from the displacement of the lower fixed jaw through a glass window of the thermostatically controlled bath by means of a travelling micrometer. The strain of the cotton yarn was negligible under our conditions. The temperature was controlled to be 90, 70, and 50 ± 0.5 °C. Silicon oil was used for creep measurements at 90 and 70 °C, whereas water was used at 50 °C because high viscosity of silicon oil at 50 °C caused a non-uniform temperature distribution in the bath. We have not shown the data at temperatures lower than 50 °C, because there was no significant difference between the values of $\dot{\varepsilon}_p$ at given stresses, when taking experimental error into account. Reproducibility of the values of $\dot{\varepsilon}_p$ at given temperatures and stresses was better than 8%: the reproducibility was better as the temperature was high. The disadvantage of the procedure adopted by us to determine the creep is the lack of elongation data less than about 60 s; until the vibration of the lower fixed jaw becomes stable when the specimen is wounded, we cannot determine elongation. We think, however, that the lack of the initial elongation data is not a serious disadvantage when evaluating the parameters in Equation 1 except for $\dot{\varepsilon}_0$, which is not evaluated in this study.

4. Results and Discussion

4.1. Identification of cholesteric liquid crystalline order in the cast films

Fig. 2 shows the polarized microphotographs of the texture for the solid cast films of EC and HPC. The films cast from liquid crystalline systems, irrespective of species of cellulose derivatives, exhibited mosaic-like texture, whereas EC-D, cast from benzene system, exhibited no texture. Although the casting conditions, chemical structures, and molecular weights were different, the textures of all EC and HPC except for EC-D were not markedly different from each other.

Fig. 3 shows the texture of liquid crystalline solutions of EC in m-cresol observed by use of polarized microscope. Compared with the textures of Figs 2 and 3, there was no marked difference. This suggests that the solid films cast from liquid crystalline solutions exhibited cholesteric liquid crystalline order.

The existence of the cholesteric liquid crystalline order in the cast films was also confirmed by performing circular dichloism [1]. Fig. 4a and b show the CD spectra for EC and HPC films, respectively. EC films exhibited a positive peak around 400 nm except for EC-D, whereas HPC films gave a negative peak around 240 nm. This finding clearly showed that all EC and HPC films except for EC-D remained of cholesteric liquid crystalline order and had different cholesteric senses: EC had a left-handed cholesteric sense and HPC a right-handed one. Most cellulose derivatives form right-handed cholesteric liquid crystals as HPC [25], whereas EC liquid crystal had been

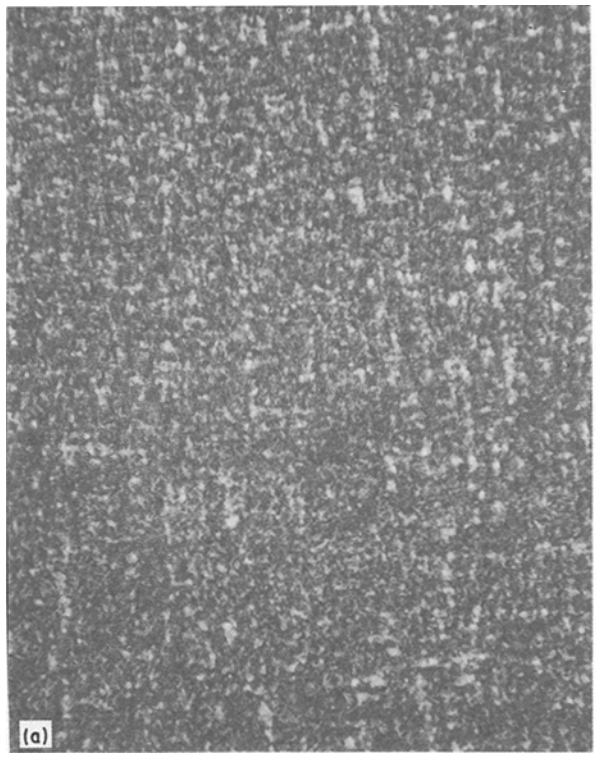

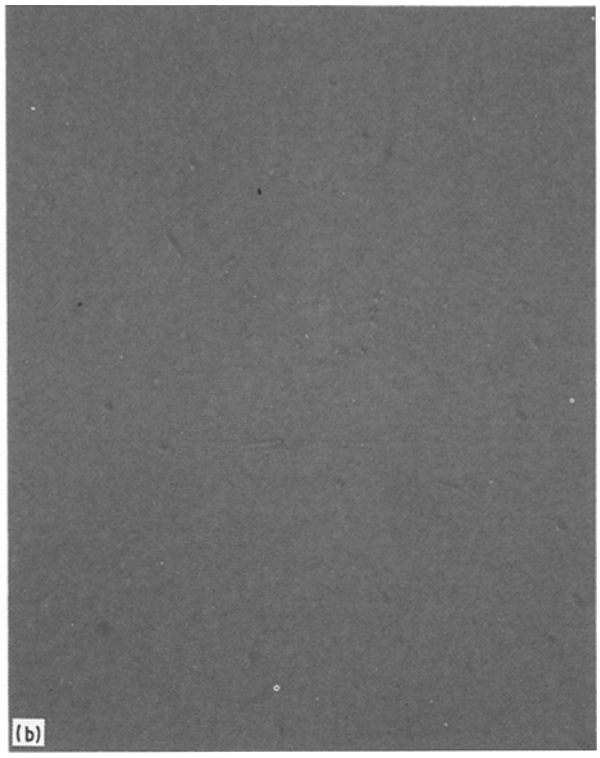

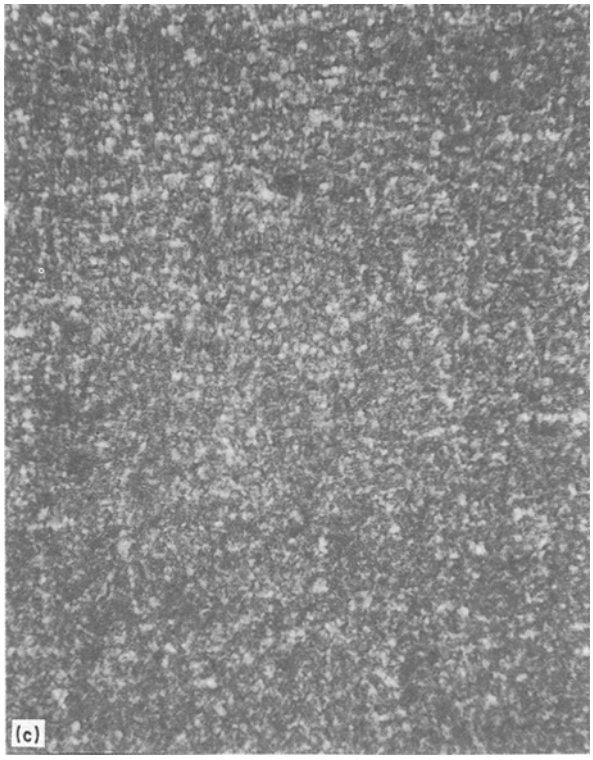

Figure 2 Polarized optical micrographs for cast films: (1) EC-B; (2) EC-D; (3) HPC-B.

observed to be left-handed [26]: the handedness of EC was dependent on solvent [25].

Fig. 5 shows H_v SALS patterns of HPC and EC films. All films except for EC-D exhibited a four-leaf clover pattern: + type pattern. This + type pattern was similar to those of HPC solid films observed by Samuels [27], Hashimoto *et al.* [28], Takahashi *et al.* [6] and was different from those of HPC solutions observed by Onogi *et al.* [29] and Meeten *et al.* [30] (× type pattern); solid films cast from liquid crystalline solutions exhibit + type pattern, whereas liquid crystalline solutions exhibit an × type pattern.

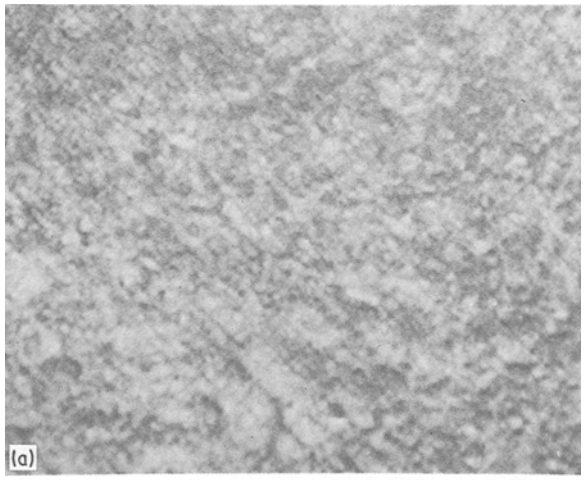

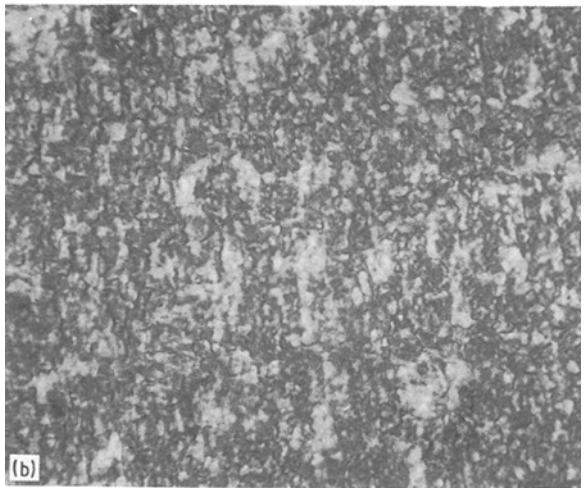

Figure 3 Polarized optical micrographs for liquid crystalline solutions: (1) EC-B/m-cresol 50 wt %; (2) HPC–DMA 50 wt %.

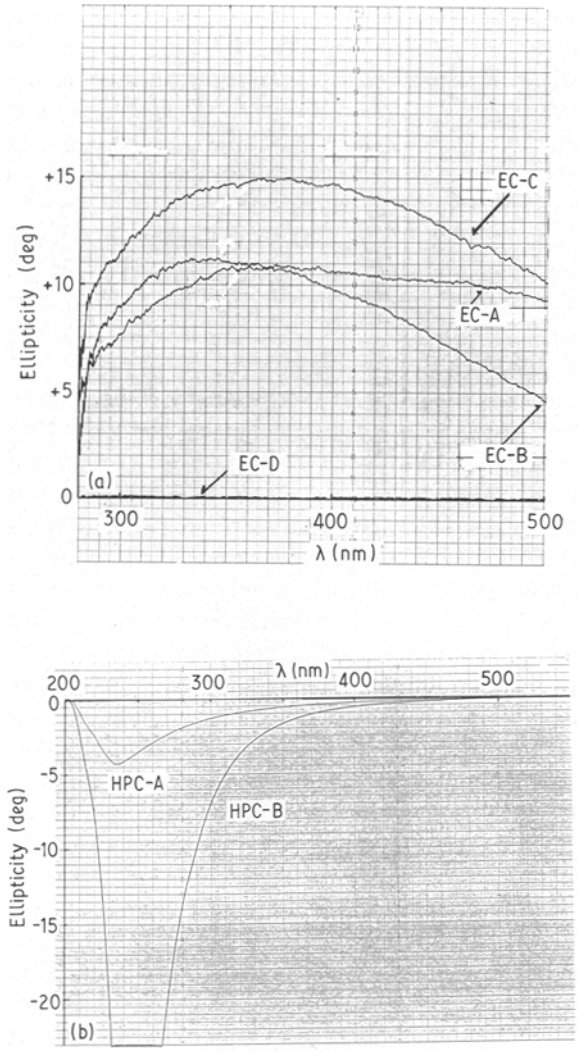

Figure 4 CD spectra for cast films: (1) EC-A, EC-B, EC-C, and EC-D; (2) HPC-A and HPC-B.

Those results shown in Figs 2, 3, 4, and 5 show that all the films except for EC-D remain of cholesteric liquid crystalline order; EC-D film is amorphous.

4.2. Creep behaviour

4.2.1. Stress dependence

Fig. 6 shows typical creep curves at given stresses at 90 °C for EC-B. The creep behaviour was general: the strain increased with time and stress [18]. A similar behaviour was observed for other films and at other temperatures. Within our experimental conditions, all films did not fail. When the same data were plotted on a scale of ε against $t^{1/3}$ (Andrade plot), the curves were not linear; there were two different linear regions.

Fig. 7 shows typical Sherby–Dorn plots (logarithm of strain rate $\dot{\varepsilon}$ against strain ε) for EC-B at 90 °C; applied stresses were the same as in Fig. 6. At each stress, the strain rate decreased with increasing strain and ultimately attained a constant level. This behaviour was observed for all other films. It was noteworthy that the decrease in the creep rate with strain for our films was very little different from that for polyethylene reported by Ward *et al.* [15–17]. The creep rate for polyethylene decreased gradually and a constant creep rate was reached: the plot displayed a downward curvature; whereas the creep rate for our films fell steeply at a given strain and was followed by an abrupt attainment of a constant level of the creep rate. The reason for the different manner in the creep rates is not clear.

The constant plateau strain rate $\dot{\varepsilon}_p$ increased with stress and showed a linear logarithmic dependence on stress. This is shown in Fig. 8 for EC-B. Consequently, our finding clearly shows that the thermally activated

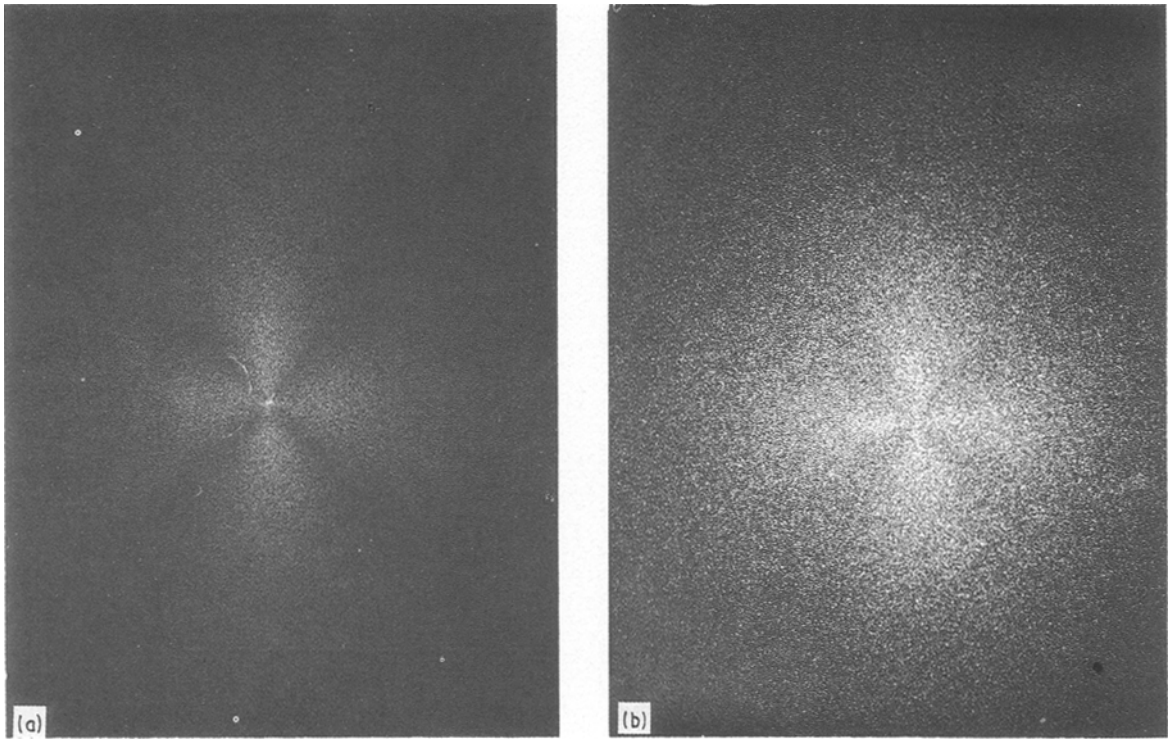

Figure 5 H_v SALS patterns for cast films: (1) EC-B; (2) HPC-B.

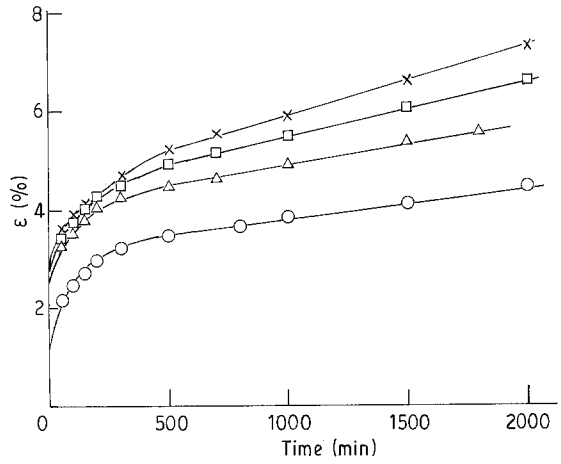

Figure 6 Creep strain plotted against time for EC-B at 90 °C; (applied stress: ○ 6.46 MPa, △ 6.85 MPa, □ 7.66 MPa, × 8.00 MPa).

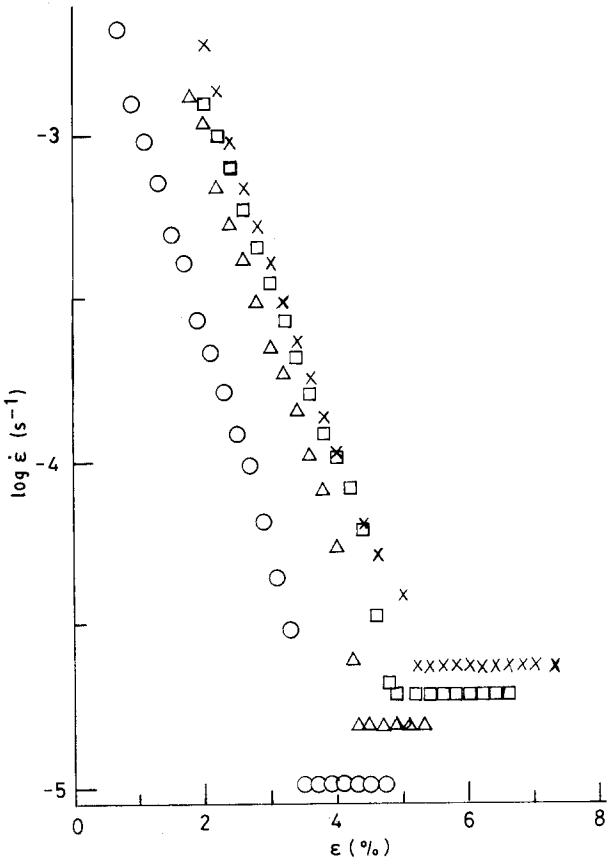

Figure 7 Typical Sherby–Dorn plot for EC-B at 90 °C; applied stress as in Fig. 6.

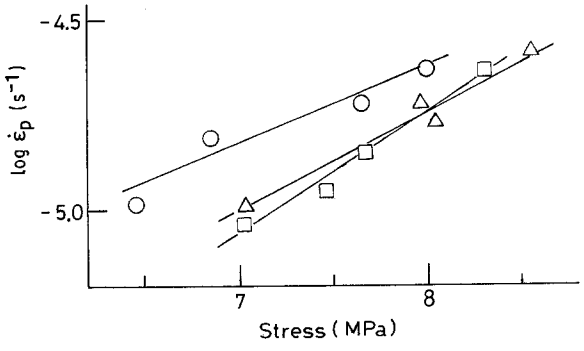

Figure 8 $\log \dot{\varepsilon}_p$ plotted against applied stress for EC-B. (Temperature: ○ 50 °C, △ 70 °C, □ 90 °C)

Eyring process can be applied to the creep behaviour of our films: Equation 1 is valid for our films. The slope of the straight line is $(V/2)\,3k$ and the value of V can be evaluated by the least-squares method: the correlation coefficients (r^2) were greater than 0.94. The values of V for all films at given temperatures are shown in Table III. The order of V for our films was 1 in nm^3. The value of V at given temperatures for EC films increased with increasing $\bar{M}_w$. Compared with EC-D (amorphous) and EC-B (liquid crystalline), which have the same $\bar{M}_w$, the value of V for EC-D was greater than that for EC-B. The value of V for EC films was greater than that for HPC films. Furthermore, the value of V for HPC film cast at − 18 °C was smaller than that for HPC film cast at room temperature. Unfortunately, there were no data on the value of V for liquid crystalline polymers other than our cellulosics. To compare our data with those for crystalline and amorphous polymers, therefore, the data for polyethylene (typical crystalline polymer) and for polymethylmethacrylate (typical amorphous polymer) are shown in Table III together with our data for EC and HPC. The value of V for EC and HPC was greater than that for polyethylene [15] and was smaller than that for polymethylmethacrylate [13]. Liquid crystalline state is generally intermediate between crystalline state and amorphous one. Our finding suggests, therefore, that the value of V decreases with increasing crystallinity. Ward *et al.* [16] have already reported that the value of V for polyethylene exhibited to decrease with increasing degree of crystal continuity: an activated event became more localized with increasing molecular alignment and perfection. Their finding supports our suggestion described above. Consequently, the activated event for EC films became more localized with increasing $\bar{M}_w$ and more localized than that for HPC films. Furthermore, the activated event for HPC film cast at − 18 °C became more localized than that for HPC cast at room temperature. With respect to the effect of casting temperature on V, we will show the data in detail for EC films in the next paper in this issue [31]: V for EC film cast at − 18 °C was smaller than that cast at room temperature.

Here we will describe the relation between the value of V and the size of liquid crystalline domains. Generally, liquid crystals are made up of polydomains [32]. Onogi *et al.* [29, 33], Bheda *et al.* [34], Fried *et al.* [35], and Meeten *et al.* [30] have reported the domain size of liquid crystalline solutions of HPC in water and organic solvents, but not the domain size in the solid films. Nishio *et al.* [9–11] have described that there were many round particles in the cast HPC and EC films and in the hot-pressed HPC films: the size of the particles was 100 to 300 nm in diameter. This size of the particles was more than two orders of magnitude smaller than that of the domain in the liquid crystalline solutions. This was consistent with the tendency that the domain size decreases with increasing concentration. Now we assume the round particle as the liquid crystalline domain in the solid films. To compare the size of the round particle and the volume of V obtained by us, we estimate the volume of the

TABLE III Activated parameters for polymers

Film	Activated volume, V (nm^3)				V_{av}	ΔU_{approx} (kcal mol^{-1})	Reference
	90 °C	70 °C	50 °C	20 °C			
EC-A	2395	1361	686	—	1481		this work
EC-B	3042	1796	849	—	1896		this work
EC-C	3768	2580	913	—	2420		this work
EC-D	4321	3821	2245	—	3460		this work
HPC-A	1267	1015	634	—	972	8.79	[21]
HPC-B	1682	1524	1169	—	1458	11.8	[21]
PE[a]				87		37	[15]
PMMA[b]				8365		48	[13]

[a] Polyethylene
[b] Polymethylmethacrylate.

round particle in the cast films of HPC. We assume, in addition, the round particle is disc shaped to simplify the estimation of the volume. The thickness of the round particle was 10 to 20 nm. The volume of the round particle was, therefore, of the order of 10^5 nm. This estimated value of the particle was far greater than the value of V determined by us, shown in Table III, even if the assumption in the shape of particle is too simple. This revealed that the value of V evaluated by using creep data did not mean the size of liquid crystalline domain. In fact the value of V decreases with increasing degree of crystal continuity [16]. This clearly suggests that the value of V does not mean the size of crystallite or crystalline domain. Consequently, the value of V was not equal to the size of liquid crystalline domain; liquid crystalline domain size is greater than the value of V and varies inversely with the value of V: the liquid crystalline domain size increases as the value of V decreases, therefore, only information obtained from the values of V for films which has comparatively a larger domain size of films. Our data show the following: (1) the size of liquid crystalline domain for EC films increased with increasing $\bar{M}_w$ and was larger than that for HPC; (2) the domain size of the HPC film cast at -18 °C was greater than that of the HPC film cast at room temperature. Furthermore, the value of V is a measure of how the activated event becomes localized. Our findings suggest, therefore, that the activated creep deformation for the liquid crystalline EC and HPC solid films does not occur at the domain boundary, but in the domain.

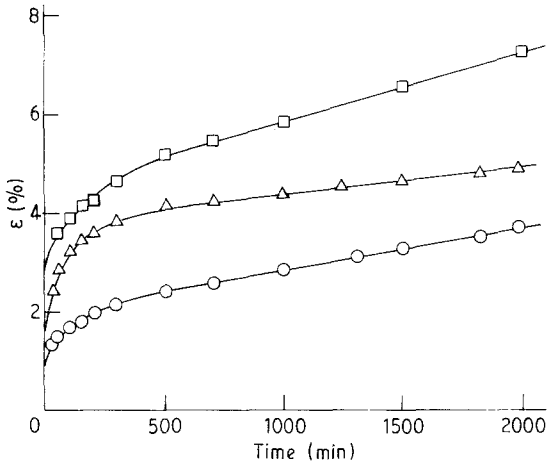

Figure 9 Creep strain plotted against time for EC-B at applied stress *ca.* 8 MPa. (Temperature: ○ 50 °C, △ 70 °C, □ 90 °C)

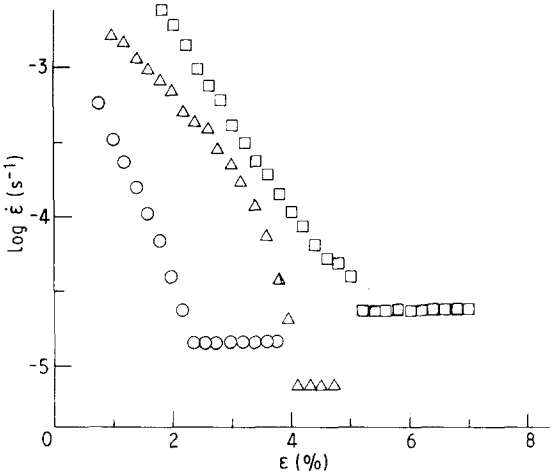

Figure 10 Sherby–Dorn plot for EC-B at applied stress *ca.* 8 MPa. (Temperature: ○ 50 °C, △ 70 °C, □ 90 °C)

4.2.2. Temperature dependence

Fig. 9 shows the creep curves for EC-B at given temperatures. This behaviour was general: the strain increased with increasing temperature at given times [18].

Fig. 10 shows the Sherby–Dorn plots at given temperatures for EC-B. The constant plateau strain rate $\dot{\varepsilon}_p$ was obtained at all temperatures. The value of V at given temperatures is shown in Table III; the value of V increased with increasing temperature. Our finding means that the size of the unit which deforms under creep increases as temperature increases: the activated event becomes less localized with increasing temperature.

Fig. 11 shows the logarithm of $\dot{\varepsilon}_p$ as a function of $1/T$ for EC-B and HPC-B. The plots for HPC were

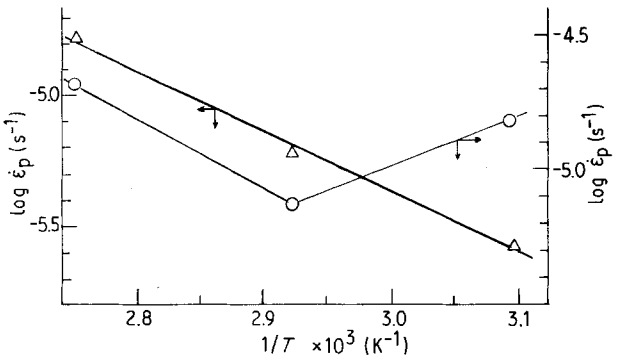

Figure 11 $\log \dot{\varepsilon}_p$ plotted against $1/T$ for cast films. (○ EC-B at applied stress of *ca.* 8 MPa, △ HPC-B at applied stress of 6 MPa)

linear, whereas those for EC were not linear. This suggests that in our experimental temperature range the activated mechanism was the same for HPC, however, was not for EC.

5. Conclusions

EC films cast from liquid crystalline solution in m-cresol remained a left-handed cholesteric liquid crystalline order, whereas EC film cast from non-liquid crystalline solution in benzene did no liquid crystalline order and was amorphous. HPC films cast from DMA system remained a right-handed cholesteric sense. The Eyring thermally activated process could be applied to the creep behaviour of our EC and HPC cast films and the activated volume of those films could be evaluated. The activated volume V was of the order of 1 nm^3 and greatly depended on the casting conditions, molecular weight, and testing temperature. The value of V for the liquid crystalline EC films was smaller than that for the amorphous EC film; the value of V for EC films increased with decreasing $\bar{M}_w$ and with increasing temperature; the value of V for EC films was greater than that for HPC films; and the value of V for HPC film cast at $-18\,^{\circ}C$ was smaller than that for HPC film cast at room temperature. Our findings suggest that the value of V tends to be smaller as the liquid crystalline order increases. The value of V evaluated by using creep data was smaller than the domain size of liquid crystalline phase.

References

1. G. CHARLET and D. G. GRAY, *Macromolecules* **20** (1987) 33.
2. A. M. RITCEY and D. G. GRAY, *Biopolymers* **27** (1988) 1363.
3. J. GIASSON, J.-F. REVOL, A. M. RITCEY and D. G. GRAY, *Biopolymers* **27** (1988) 1999.
4. S. SUTO, M. KUDO and M. KARASAWA, *J. Appl. Polym. Sci.* **31** (1986) 1327.
5. S. SUTO, M. OHSHIRO, W. NISHIBORI, H. TOMITA and M. KARASAWA, *ibid.* **35** (1988) 407.
6. J. TAKAHASHI, K. SHIBATA, S. NOMURA and M. KUROKAWA, *Sen-i Gakkaishi* **38** (1982) T-375.
7. K. SHIMAMURA, *Makromol. Chem. Rapid Commun.* **4** (1983) 107.
8. M. HORIO, S. ISHIKAWA and K. ODA, *J. Appl. Polym. Sci. Appl. Polym. Symp.* **41** (1985) 269.
9. Y. NISHIO, T. YAMANE and T. TAKAHASHI, *J. Polym. Sci. Polym. Phys. Ed.* **23** (1985) 1053.
10. Y. NISHIO and T. TAKAHASHI, *J. Macromol. Sci.-Phys.* **B23** (1984–85) 483.
11. Y. NISHIO, S. SUSUKI and T. TAKAHASHI, *Polym. J.* **17** (1985) 753.
12. G. HALSEY, H. J. WHITE and H. EYRING, *Text. Res. J.* **15** (1945) 295.
13. O. D. SHERBY and J. E. DORN, *J. Mech. Phys. Solid* **6** (1958) 145.
14. M. J. MINDEL and N. BROWN, *J. Mater. Sci.* **8** (1975) 863.
15. M. A. WILDING and I. M. WARD, *Polymer* **22** (1981) 870.
16. I. M. WARD and M. A. WILDING, *J. Polym. Sci. Polym. Phys. Ed.* **22** (1984) 256.
17. M. A. WILDING and I. M. WARD, *J. Mater. Sci.* **19** (1984) 629.
18. M. H. LAFITTE and A. R. BUNSELL, *Polym. Eng. Sci.* **25** (1985) 182.
19. R. H. ERICKSEN, *Polymer* **26** (1985) 733.
20. S. SUTO, K. OIKAWA and M. KARASAWA, *Polym. Commun.* **27** (1986) 262.
21. S. SUTO, T. IWAYA and M. KARASAWA, *Sen-i Gakkaishi* **45** (1989) 135.
22. C. J. CLEMETT, *Anal. Chem.* **45** (1973) 186.
23. F. F-L. HO, R. R. KOHLER and G. A. WARD, *ibid.* **44** (1972) 178.
24. S. SUTO, M. OHSHIRO, R. ITO and M. KARASAWA, *Polymer* **28** (1987) 23.
25. J.-X. GUO and D. G. GRAY, *Macromolecules* **22** (1989) 2082.
26. U. VOGT and P. ZUGENMAIER, *Ber. Bunsen-Ges. Phys. Chem.* **89** (1985) 1217.
27. R. J. SAMUELS, *J. Polym. Sci. A* **7** (1969) 1197.
28. T. HASHIMOTO, S. EBISU and H. KAWAI, *J. Polym. Sci. Polym. Phys. Ed.* **19** (1981) 59.
29. Y. ONOGI, J. L. WHITE and J. F. FELLERS, *ibid.* **18** (1980) 663.
30. G. H. MEETEN and P. NAVARD, *ibid.* **26** (1988) 413.
31. S. SUTO, K. OIKAWA, T. IWAYA and M. KARASAWA, *J. Mater. Sci.*, following paper in this issue.
32. T. ASADA, H. MURAMATSU, R. WATANABE and S. ONOGI, *Macromolecules* **13** (1980) 867.
33. Y. ONOGI, J. L. WHITE and J. F. FELLERS, *J. Non-Newt. Fluid Mech.* **7** (1980) 121.
34. J. BHEDA, J. F. FELLERS and J. L. WHITE, *Colloid Polym. Sci.* **258** (1980) 1335.
35. F. FRIED and P. SIXOU, *J. Polym. Sci. Polym. Chem. Ed.* **22** (1984) 239.

Received 29 May
and accepted 26 June 1990